

# High Performance Supercapacitors Based on Mesopore Structured Multiwalled Carbon Nanotubes

Yang Xu,<sup>[a]</sup> Weili Shi,<sup>\*[a]</sup> Ruguang Li,<sup>[a]</sup> Zheng Qiao,<sup>[a]</sup> Jian Fang,<sup>[a]</sup> Quanlin Yang,<sup>[b]</sup> and Chuanxi Xiong<sup>[b]</sup>

A 3D CNT/few layered graphene construct (CNT–FLG) with mesopore structure was fabricated and applied in supercapacitors. The structure was acquired through a two-step method. Firstly, commercial multiwalled carbon nanotubes (MCNTs) were oxidized in a mixed solution of concentrated acid and modified with a couple of long-chain organic ions. Second, the above resultant product was carbonized at a high temperature. The achieved structure offers a 3D interconnected electrically conductive network as well as mesopore structure. It also

significantly improves the specific surface area of MCNTs. Result of BET tests showed that the specific surface area of CNT–FLG reached to 2235 m<sup>2</sup>/g. When acted as electrode materials in a supercapacitor structure, specific capacitance was approximately 531.2 F/g at a current density of 0.8 A/g. At current density of 50 A/g, specific capacitance remained 204.4 F/g. Besides, the capacitance retention was as high as 96.18% after 10000 cycles at the current density of 5 A/g.


## 1. Introduction


The growing number of electronic devices, powering electromobility or hybrid electromobility demand efficient energy storage as well as high power density, high rate capability and long term stability.<sup>[1–3]</sup> Compared with numerous kinds of energy storage devices, the most promising candidates seems to be supercapacitor because of their excellent performance, superior cycle lifetimes, safety and environmentally friendly properties.<sup>[4–7]</sup> Electrochemical double layered capacitors (EDLC) have also called the attentions of researchers worldwide. Their energy storing process is a physical process based on the formation of a double-layer formation occurring at the surface of the electrodes. Thus, acquiring high-performance EDLC would require that electrode materials have high specific surface area and well-controlled structure.<sup>[8–10]</sup> Due to their extraordinary conductivity, fine corrosion resistance, high temperature stability, mechanical and electrochemical capabilities, carbon nanotubes (CNTs) are considered an ideal choice for electrodes in electric double layer capacitors (ECs).<sup>[11–13]</sup> Nevertheless, there are many factors impede potential applications of CNTs as electrode structure for ECs.<sup>[14]</sup> For example, CNT

aggregation can decrease its specific surface area, discontinuous pores may also lead to poor interface connect between electrodes and current collector. As a consequence, these disadvantages restrict the electrochemical performance of CNT.<sup>[15,16]</sup> To elevate electrochemical property of CNT supercapacitors, many researchers tend to use vertically aligned CNTs.<sup>[17–19]</sup> In this work, we first used a mixture of concentrated acid to oxidize the surface of multiwalled carbon nanotubes (MCNTs), then oxidized MCNTs were modified by some long-chain organic ions through surface oxygen containing groups. By doing so, it could make MCNTs untangled and well-dispersed. At last the above resultant product was carbonized at a high temperature under the nitrogen gas protection, achieving a 3D carbon nanotube structure combined with layered graphene (CNT–FLG). This architecture could not only significantly improve the specific surface area of MCNTs but also provide a 3D interconnected electrically conductive network and mesopore structure. It was applied to supercapacitor as electrode materials, the CNT–FLG electrode exhibited excellent electrochemical performance in comparison with pristine MCNTs (p-MCNTs) electrode. The BET test results revealed an amazing specific surface area which is 2235 m<sup>2</sup>/g for CNT–FLG. What's more, specific capacitance was approximately 531.2 F/g at current density of 0.8 A/g. It remains to be 204.4 F/g at current density around 50 A/g. Besides, its capacitance retention was as high as 96.18% after 10000 cycle time at a current density of 5 A/g. The superior electrochemical performance of CNT–FLG supercapacitors demonstrates an effective strategy for preparing high efficiency energy storage devices.

[a] Y. Xu, W. Shi, R. Li, Z. Qiao, J. Fang  
Huanggang Normal University  
Xingang 2nd Avy  
Huanggang 438000 (China)  
E-mail: shiweili@hgnu.edu.cn

[b] Q. Yang, C. Xiong  
Wuhan University of Technology  
Luoshi Road 122  
Wuhan 430070 (China)

 Supporting information for this article is available on the WWW under <https://doi.org/10.1002/open.202000274>

 © 2021 The Authors. Published by Wiley-VCH GmbH. This is an open access article under the terms of the Creative Commons Attribution Non-Commercial NoDerivs License, which permits use and distribution in any medium, provided the original work is properly cited, the use is non-commercial and no modifications or adaptations are made.

## 2. Results and Discussion

The detailed experiment process and the formation mechanisms for CNT–FLG can be seen in our previous work.<sup>[22]</sup> The

microstructure of fabricated is presented in Figure 1 2 and 3, it can be observed from Figure 1a that pCNT is shown as dispersed long tubes. CNTF in Figure 1b shaped as folded planes. Figure 1c shows SEM image of carbonized CNTF, which is shorter and thinner than that of pCNT.

MCNTs in CNT–FLG is formed into a compact porous structure, which is evidently different from the untreated or only oxidized MCNTs in previous reported work.<sup>[23–25]</sup> Figure 2b–c were the high-magnification TEM images of the integrated CNT–FLG. Figure 2b–c indicates that Ultrathin carbon layers has been connected between MCNTs as Figure 2a shows. These results were consistent with our previous report.

To further investigate the carbon layers, it was first grinded, then dissolved in NMP to and subject to an ultrasonic process for several minutes. Figure 3 a–c were the TEM images of CNT–FLG sample after strictly grinding and ultrasonic processing. The typical spacing of  $\sim 0.34$  nm lattice fringes can be seen from the destroyed CNT–FLG structure (Figure 3c). It's worth noticing that the layers of the produced FLG were not uniform.

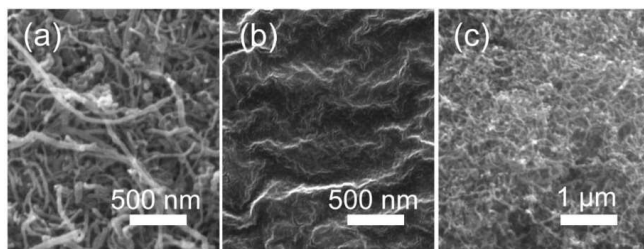


**Figure 1.** Surface SEM images of (a) parent CNTs, (b) CNTF and (c) carbonized CNT.

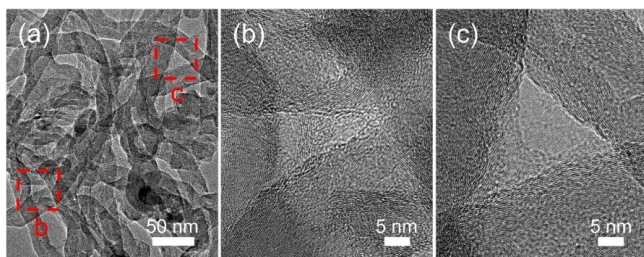


**Figure 2.** TEM images of (a) polydispersed CNTs, high magnification TEM images (b–c) of CNT–FLG samples.

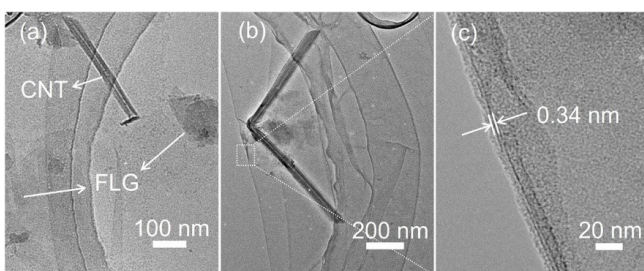


**Figure 3.** low magnification TEM images (a–c) of CNT–FLG sample after strictly grinding and ultrasonic processing.

But this has little impact on the electrochemical properties of CNT–FLG electrodes.

The AFM images were carried out for characterization of the produced FLG in CNT–FLG structure thickness. The results of AFM were given in supplementary information Figure S1. Both the MCNTs and FLG could be observed in Figure S1, and the thickness of FLG were 2.3 nm and 6.6 nm respectively. According to the definition of graphene mentioned in literature, such carbon layers between the MCNTs can be defined as few-layer graphene,<sup>[26]</sup> some parts of the graphene are multilayered. More characterizations of AFM results can be found in a previous report.<sup>[22]</sup>

The Raman spectroscopy and X-ray diffraction (XRD) analysis were performed for identification of the fabricated CNT–FLG respectively. AFM results were given in supplementary information Figure S1. The Raman spectra revealed that the peak at about  $1604\text{ cm}^{-1}$  matching D' peak of graphene were appeared.<sup>[27,28]</sup> D' peak is a readable defect peak of graphene due to its armchair edges and zigzag edges. However, CNT structurally comes out from curled graphene, in which these edges is gradually fixed. Therefore, the D' peak intensity of CNT was greatly reduced and not obvious. We can't find any broad peak at  $\sim 1500\text{ cm}^{-1}$ , which indicates amorphous carbon's absence (Figure S2a).<sup>[29,30]</sup> These results confirmed again there were graphene flakes produced but no amorphous carbon present. Figure S2b compared the XRD curves of p-MCNTs, CNTF and CNT–FLG. CNTF sample presented a broad peak at  $\sim 20.8^\circ$ , attributing existence of amorphous carbon.<sup>[29]</sup> While that broad peak was not appeared for CNT–FLG sample, it again supporting the consequence from Raman spectra.

Since supercapacitors have high power density, rapid charging/discharging as well as longer cycle number features, it is well known as potential energy storage devices so far. However, excellent performance of supercapacitors are limited by its surface area ratio and well-controlled, structural optimized active electrode material.<sup>[31,32]</sup> In our research, fabricated CNT–FLG connect 1D CNTs combined with 2D few-layered graphene could provide 3D interconnected electrically conductive networks together with massive available surface areas. Such structure can be positive for charge transport ability. Specific surface area together with pore size distributions of CNT–FLG and p-MCNTs were shown in Figure 4. Specific surface area of CNT–FLG went to  $2230\text{ m}^2/\text{g}$  from BET test, which was about 5 times than p-MCNTs ( $471\text{ m}^2/\text{g}$ ) samples. In addition, comparing with pore-size distribution of CNT–FLG and p-MCNTs (Figure 4b and 4c), it was found that pore-size distribution of CNT–FLG were among the range of 2 to 50 nm, thus indicating hierarchically porous structure was successfully formed and most of the pores were belonged to mesopores. While most pore-size distribution of p-MCNTs were in the range of less than 15 nm.

The electrochemical performance of CNT–FLG as the electrode materials of supercapacitor were investigated using a three-electrode test system. For comparison, p-MCNTs as well as physical mixture of CNT and FLG were also prepared as the electrode materials of supercapacitor using the same method. Figure 5a showed the CV curves of CNT–FLG electrode at scan

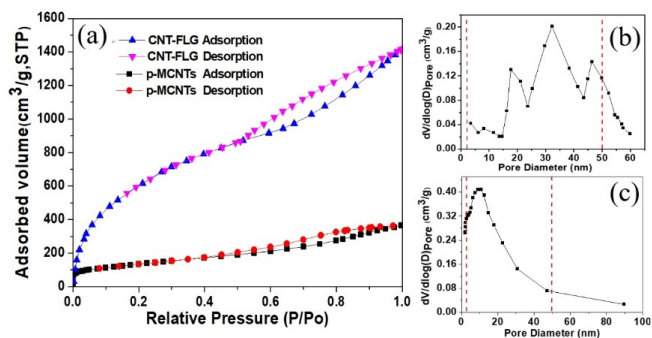


**Figure 4.** (a) N<sub>2</sub> adsorption/desorption isotherms of CNT-FLG and p-MCNTs samples. (b) Pore size distribution of CNT-FLG. (c) Pore size distribution of p-MCNTs.

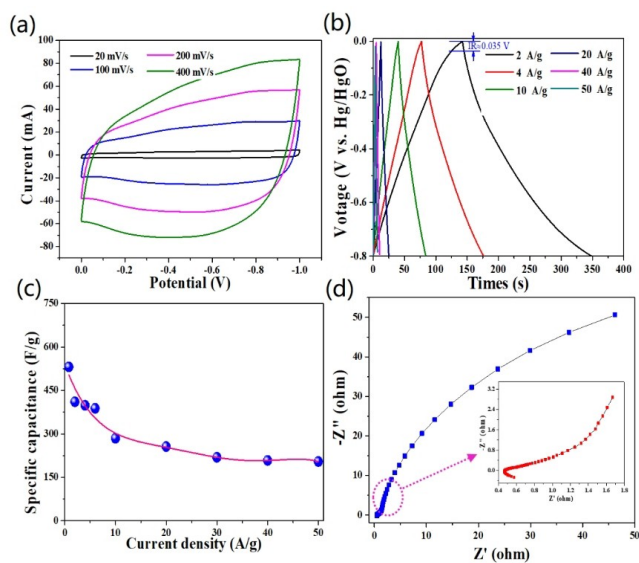


**Figure 5.** Electrochemical properties of CNT-FLG electrode. (a) CV curves of CNT-FLG electrode vary with various scan rates. (b) Charge/discharge curves for CNT-FLG electrode under various current densities. (c) Specific capacitance varies with different current densities. (d) Nyquist plot for CNT-FLG electrode.

rates of 20, 100, 200, 400 mV/g respectively. All curves presented nearly rectangular shapes at various scanning rates. Besides, no obvious redox peaks were appeared, which illustrated the CNT-FLG supercapacitor behavior mainly dominated by double layer capacitor (EDLC), almost no pseudo-capacitance existence. This further implied the oxygen-containing groups grafted on p-MCNTs were almost completely carbonized. From picture of Figure 6a and Figure S3a, the presented CV curves of p-MCNTs and physical mixture of CNT and FLG electrode were analogous to “boat” shapes rather than rectangle shapes at different scanning rates, and there is also no obvious redox peaks, which maybe result from the oxygen-containing groups were too few to participate in charge/discharge reaction.

Galvanostatic charge/discharge curves of CNT-FLG electrode under various current densities from 2 to 50 A/g was presented in Figure 5b. Charge/discharge curves presented

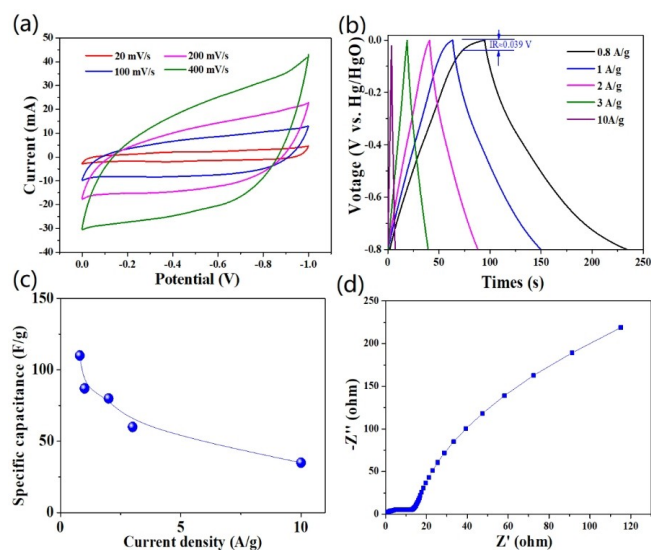


**Figure 6.** Electrochemical measurements of p-MCNTs. (a) Variation of CV curves under different scan rates. (b) Charge/discharge curves for p-MCNTs electrode under various current densities. (c) Specific capacitance varies with different current densities. (d) Nyquist plot for p-MCNTs.

symmetry triangular shapes. Even at lower current density, the charge/discharge curve of CNT-FLG electrode was still symmetry and the IR drop were smaller compared with the curve of p-MCNTs electrode (Figure 6b), which illustrated CNT-FLG electrode had a better reversible charge-discharge performance than p-MCNTs electrode. This result was similar with that of CV curves.

The specific capacitance of electrode (C) was measured using equation 1. Where  $I$  represent current density,  $m$  stands for the mass of active material,  $\Delta t$  was discharge time and  $\Delta V$  was used as voltage range after the IR fell during discharging period. Figure 5c, Figure 6c and Figure S3c were presented as variation in specific capacitance of CNT-FLG and p-MCNTs electrodes as a function of current density respectively. Specific capacitance of CNT-FLG electrode was as high as 531 F/g at a current density of 0.8 A/g. It is about 5 times than the value of p-MCNTs (110 F/g), also about 5 times than the value of physical mixture of CNT and FLG (Figure S3c). The specific capacitance of CNT-FLG, p-MCNTs and physical mixture of CNT and FLG electrodes decreased with the rise of current density as expected. What should be mentioned is that at a huge current density of 10 A/g, the specific capacitance of CNT-FLG electrode still remained at about 285 F/g, while specific capacitance of p-MCNTs electrode reduced to only 35 F/g, specific capacitance of physical mixture of CNT and FLG (Figure S3b) electrode dropped to only 35 F/g, Furthermore, even at the largest testing current density of 50 A/g, CNT-FLG electrode still exhibited a remarkable specific capacitance of 204 F/g. Such outcomes displayed above indicated that the CNT-FLG electrode performance was significantly improved in comparison with p-MCNTs samples and physical mixture of CNT and FLG in specific capacitance as well as rate capability. What's more, the charging times for CNT is about 40s at 2 A/g, charging times for CNT-FLG is 140s at 2 A/g. However, taking

equation 1 into consideration. Specific capacitance of CNT electrode was  $\sim 80$  F/g, while that of CNT-FLG is more than 375 F/g. The charging speed of CNT-FLG is  $\sim 33\%$  faster than that of CNT. Claiming the fact that CNT-FLG sample exhibit better electrochemical property. These outstanding capacity of CNT-FLG electrode is owing to its unique structural features: (1) large accessible surface areas could provide more active sites and space for ion adsorption, which resulted in an increased specific capacitance. (2) 3D interconnected electrical conductive networks could shorten the ion transport distance facilitating diffusion speed of electrolyte ions in the channels. Thus, the rate capability achieved remarkable improvement.

The capacitive behavior of CNT-FLG, p-MCNTs and physical mixture of CNT and FLG electrodes were characterized by electrochemical impedance spectroscopy in Figure 5d, Figure 6d and Figure S3d. Nyquist plot of CNT-FLG electrode revealed that there was almost no semicircle appeared during high-frequency part, while Nyquist plots of p-MCNTs and physical mixture of CNT and FLG electrodes showed tiny semicircles during high-frequency part, since large semicircles observed for these electrodes are attributed to the poor electrical conductivity of these materials in other literature. Therefore, conductivity of these materials can be ordered as CNT-FLG > Mix > p-MCNTs. During the low-frequency part, slopes of straight line for the CNT-FLG electrode were much higher than p-MCNTs and mixed electrodes, which illustrated the ions diffusion speed between the electrode and electrolyte interface was notably promoted. Thus, the CNT-FLG supercapacitor behaved more nearly ideal capacitive response and had higher rate capability. The results again confirmed the above conclusions.

Cycle performance was another necessary factor for electrode materials in a supercapacitor. Cycle property of CNT-FLG electrode was measured under 5 A/g for 10000 charge-discharge round. Value of specific capacitance was measured every 200 times based on the equations of  $C = \Delta Q / \Delta V$ . The variation in specific capacitance as a function of cycle numbers was shown in Figure 7.

What should be noted is that the initial specific capacitance of CNT-FLG electrode was closed to 400 F/g, which was

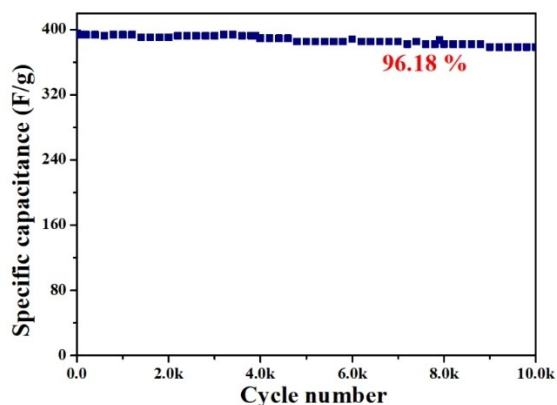


Figure 7. The electrochemical stability at current density of 5 A/g over 10000 cycle times.

significantly higher than previous reports based on EDLC that use other carbon materials<sup>[31–35]</sup> as Figure 8 shows. Moreover, the capacitance retention remained to be 96% of its original value over 10000 cycle times, which indicated that CNT-FLG as the electrode materials of supercapacitor possessed excellent cycling stability and was suitable for preparing high efficiency energy storage supercapacitors.

## Experimental Section

### Fabricating process of 3D CNT/few layered graphene structure

3D CNT/few layered graphene architectures were fabricated through two steps. First, the MCNTs was modified by a couple of positive and negative long-chain organic ions ( $[(\text{CH}_2\text{O})_3\text{Si}(\text{CH}_2)_3\text{N}^+(\text{CH}_3)_2\text{C}_{18}\text{H}_{37}\text{Cl}^-]$  and  $[\text{C}_9\text{H}_{19}\text{C}_6\text{HO}(\text{CH}_2\text{CH}_2\text{O})_{10}\text{SO}_3^- \text{K}^+]$ ) to synthesize CNT fluids without solution (CNTF). Before modification, MCNTs must be treated by a mixed solution of concentrated  $\text{H}_2\text{SO}_4/\text{HNO}_3$  (ratios of the volume was 3:1). The detailed procedures can be seen from our previous reported work.<sup>[20,21]</sup> Second, transferred the as-prepared CNTF into a ceramic boat, then put it into a horizontal tube furnace and heat to  $700^\circ\text{C}$  with  $5^\circ\text{C}/\text{min}$  rate and remain for 4 h under nitrogen gas protection, after dropping to room temperature, 3D CNT/few layered graphene architecture (CNT-FLG) were obtained. For physical mixture of CNT and FLG, A mixture of CNT and FLG (ratios of the mass was 8:2) was prepared for control experiment.

### Electrochemical measurements

A CHI 660E electrochemical workstation was used to measure electrochemical performance of the samples. We use a three-electrode system with a  $6\text{ mol}\cdot\text{L}^{-1}$  KOH aqueous solution for supercapacitor tests. In our three-electrode measurement, Pt foil and Hg/HgO electrode was act as counter electrode and reference electrode respectively. Work electrode was assembled with a mixed CNT-FLG/PVDF (ratios of the mass was 9:1) in N-methyl-2-pyrrolidone (NMP) solvent. The mixed solution was coated onto Ni foam with a brush and then dried under  $60^\circ\text{C}$ . For comparison, same method for MCNTs working electrode and physical mixture of CNT and FLG working electrode were used. Charge/discharge test was performed through a voltage range of  $-0.8\sim 0\text{ V}$ . The cyclic voltammetry (CV) tests was conducted with a sweep rate of  $5\sim$

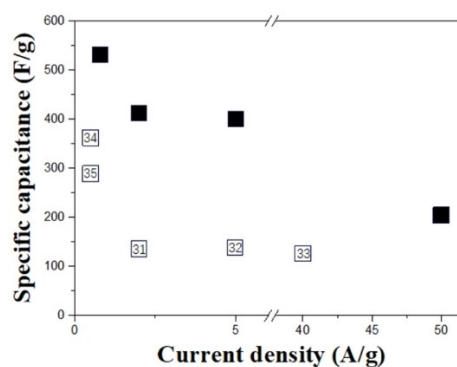


Figure 8. Comparison with other reports based on EDLC that use other carbon materials.

200 mV·L<sup>-1</sup> at a potential range of -1~0 V. For EIS tests, frequency range was set from 0.1 to 10<sup>5</sup> Hz.

### 3. Conclusions

The surface of MCNTs has been modified by organic oligomer ion pairs, and the resultant product was carbonized at a high temperature to achieve a novel 3D carbon nanotube-graphene structure (CNT-FLG). This structure is provided with a large accessible surface area and 3D interconnected electrically conductive networks. The result of BET test showed the specific surface area of CNT-G achieved 2235 m<sup>2</sup>/g. It was applied to supercapacitor as electrode materials, the CNT-FLG electrode exhibited higher specific capacitance and rate capability, more nearly ideal capacitive behaviors and excellent cycling stability in comparison with p-MCNTs electrode. This report indicates that such extraordinary electrochemical ability of CNT-FLG supercapacitors are suitable for manufacturing of high-efficiency energy storage devices and have great implications for extending supercapacitors using MCNTs as electrode materials in high-power field applications. It is also expected for further improvement for electrochemical performance of supercapacitors by optimizing CNT-FLG structure and quality.

### Acknowledgments

The authors acknowledge financial support from National Natural Science Foundation of China (51673154 and 51703177), Natural Science Fund of Hubei Province (2019CFC837), Education Fund of Hubei Province (B2020167).

### Conflict of Interest

The authors declare no conflict of interest.

**Keywords:** 3D carbon-based materials · electrode materials · organic oligomers · multiwalled carbon nanotubes · supercapacitors

- [1] H. Zhao, L. Liu, *Adv. Sci.* **2017**, *4*(10), 1700188.
- [2] M. Sessolo, H. J. Bolink, *Science*. **2015**, *350*(6263), 917–917.
- [3] Y. S. Zhou, Y. C. Zhu, *J. Mater. Chem. A*, **2018**, *6*, 14065–14068.
- [4] J. R. Miller, P. Simon, *Science*. **2008**, *321*(5889), 651–652.
- [5] A. Yu, V. Chabot, *Electrochemical supercapacitors for energy storage and delivery: fundamentals and applications*, CRC press, **2013**.
- [6] A. Afif, S. M.H Rahman, *J. Energy Storage* **2019**, *25*, 100852.
- [7] R. K. Mishra, M. Krishnaih, *Mater. Lett.* **2019**, *236*, 167–170.
- [8] M. Yang, Z. Zhou, *Adv. Sci.* **2017**, *4*(8), 1600408.
- [9] L. H. Hess, L. Wittscher, *Phys. Chem. Chem. Phys.* **2019**, *21*(18), 9089–9097.
- [10] N. Liang, Y. Ji, *J. Power Sources* **2019**, *423*, 68–71.
- [11] Y. S. Zhou, P. Jin, *J. Mater. Chem. A*. **2017**, *5*, 16595–16599.
- [12] J. N. Coleman, U. Khan, *Adv. Mater.* **2006**, *18*(6), 689–706.
- [13] Y. S. Zhou, J. Jin, *Ionics*. **2019**, *25*, 4031–4035.
- [14] L. Basirico, G. Lanzara, *Nanotechnology*. **2012**, *23*(30), 305401.
- [15] B. Kim, H. Chung, *Nanotechnology*. **2012**, *23*(15), 155401.
- [16] M. V. Kiamahalleh, S. H. S. Zein, *NANO* **2012**, *7*(02), 1230002.
- [17] X. Wang, T. Wang, *Nano Res.* **2019**, 1–16.
- [18] C. Cao, Y. Zhou, *Adv. Energy Mater.* **2019**, *9*(22), 1900618.
- [19] Y. S. Zhou, Y. C. Zhu, *Chem. Commun.* **2019**, *55*, 4083–4086.
- [20] Q. Li, L. Dong, *ACS Nano*. **2010**, *4*, 5797–5806.
- [21] Y. Lei, C. Xiong, *J. Am. Chem. Soc.* **2008**, *130*, 3256–3257.
- [22] W. L. Shi, J. Chen, *J. Phys. Chem. C*. **2016**, *120*(25), 13807–13814.
- [23] R. A. DiLeo, B. J. Landi, *J. Appl. Phys.* **2007**, *101*(6), 064307.
- [24] V. Datsyuk, M. Kalyva, *Carbon*. **2008**, *46*(6), 833–840.
- [25] L. Li, L. I. Feng, *New. Carbon. Mater.* **2011**, *26*(3), 224–228.
- [26] A. Bianco, H. M. Cheng, *Carbon*. **2013**, *65*, 1–6.
- [27] A. C. Ferrari, D. M. Basko, *Nat. Nanotechnol.* **2013**, *8*(4), 235.
- [28] M. S. Dresselhaus, A. Jorio, *Nano Lett.* **2010**, *10*(3), 751–758.
- [29] N. M. J. Conway, A. C. Ferrari, *Diamond Relat. Mater.* **2000**, *9*(3), 765–770.
- [30] A. C. Ferrari, J. Robertson, *Phil. Trans. R. Soc. A* **2004**, *362*(1824), 2477–2512.
- [31] Y. J. Kang, H. Chung, *Nanotechnology*. **2012**, *23*(6), 065401.
- [32] B. Kim, H. Chung, *Nanotechnology*. **2012**, *23*(15), 155401.
- [33] R. Yan, T. Heil, *Adv. Sustainable Syst.* **2017**, 1700128.
- [34] J. Song, W. Shen, *ChemElectroChem* **2018**, *5*(11), 1451–1458.
- [35] X. Xu, Y. Liu, *Electrochim. Acta.* **2016**, *193*, 88–95.

Manuscript received: September 15, 2020

Revised manuscript received: December 18, 2020